Geomechanics and Engineering, *Vol. 20, No. 2 (2020) 131-146*
DOI: https://doi.org/10.12989/gae.2020.20.2.131

Determination of seismic hazard and soil response of a critical region in Turkey considering far-field and near-field earthquake effect

Yetis Bulent Sonmezer*[1] and Murat Celiker[2a]

[1]*Department of Civil Engineering, Faculty of Engineering, Kirikkale University, 71450 Kirikkale, Turkey*
[2]*9th Regional Directorate, General Directorate of State Hydraulic Works, 23200 Elazig, Turkey*

(Received October 29, 2019, Revised January 7, 2020, Accepted January 10, 2020)

Abstract. Evaluation of earthquake impacts in settlements with a high risk of earthquake occurrence is important for the determination of site-specific dynamic soil parameters and earthquake-resistant structural planning. In this study, dynamic soil properties of Karliova (Bingol) city center, located near to the intersection point of the North Anatolian Fault Zone and the East Anatolian Fault Zone and therefore having a high earthquake risk, were investigated by one-dimensional equivalent linear site response analysis. From ground response analyses, peak ground acceleration, predominant site period, 0.2-sec and 1-sec spectral accelerations and soil amplification maps of the study area were obtained for both near-field and far-field earthquake effects. The average acceleration spectrum obtained from analysis, for a near-field earthquake scenario, was found to exceed the design spectra of the Turkish Earthquake Code and Eurocode 8. Yet, the average acceleration spectrum was found to remain below the respective design spectra of the two codes for the far-field earthquake scenario. According to both near- and far-field earthquake scenarios in the study area, the low-rise buildings with low modal vibration durations are expected to be exposed to high spectral acceleration values and high-rise buildings with high modal vibration durations will be exposed to lower spectral accelerations. While high amplification ratios are observed in the north of the study area for the near-distance earthquake scenario, high amplification ratios are observed in the south of the study area for the long-distance earthquake scenario.

Keywords: site response analysis; far-field effect; near- field effect; local soil conditions; Karlıova

1. Introduction

In the last decades, major earthquakes including 1999 İzmit (M=7.2), 2003 Bingol (M=6.4), 2011 Van (M=7.2) and 2017 Bodrum/Mugla (M=6.5) earthquakes, which caused casualties and had devastating effects leading to economic and sociological traumas to the nation, took place in Turkey. One of the main reasons increasing destructive effects of earthquakes is local ground conditions. Local soil conditions have long been considered an important factor affecting the impacts of severe ground motions. Seismic hazard assessments, which are conducted for evaluating the effects of local ground conditions on ground motions, can be realized for large geographical regions. As more ground motion data are collected in these assessments, local soil conditions emerge as an important factor controlling the change in ground motion and the seismic hazard specific to the region for a given earthquake. In order to reduce the destructive effects of earthquakes and to determine safer areas for settlement, studies taking local soil conditions into account have been conducted around the globe (Shiuly and Narayan 2012, El-Hady *et al.* 2012, Eskişar *et al.* 2014, Kienzle *et al.* 2006, Shafiee *et al.* 2011). Main studies on this subject are summarized below.

Cavallaro *et al.* (2008), carried out a detailed study on an area of Monte Po Hill, located in the north east of the Italian city of Catania, with a high risk of earthquake occurrence. They estimated the ground response history and response spectra of the region by performing equivalent linear seismic response analysis with the developed one-dimensional computer code. In addition, they showed that a two-dimensional model of the area under consideration can be possibly developed with the data obtained from the equivalent linear soil behavior analysis. Grasso and Maugeri (2009), performed one-dimensional equivalent linear and two-dimensional linear analyses on representative soil profiles and obtained the surface peak ground acceleration and spectral acceleration values of Catania (Italy) by adopting the earthquake that occurred on January 11th, 1693 as the maximum scenario earthquake. The city of Catania was divided into several different regions according to the peak ground acceleration and microzonation maps were created.

Edinçliler and Tuncay (2018) conducted one-dimensional equivalent linear and nonlinear soil behavior analyses to determine local soil conditions for a specific region in the Bodrum district of Mugla (Turkey). The spectral acceleration and peak ground acceleration values obtained from the equivalent linear and nonlinear analyses using two different earthquake records for two different regions were compared. They proposed that the field effects obtained from these analyses should also be taken into account in seismic designs to avoid earthquake damage.

Tavakoli *et al.* (2016) conducted soil behavior analyses

∗Corresponding author, Ph.D.
E-mail: bsonmezer@kku.edu.tr
[a]Ph.D., Engineer

Copyright © 2020 Techno-Press, Ltd.

ISSN: 2005-307X (Print), 2092-6219 (Online)

using experimental and numerical methods in order to reduce the uncertainties regarding earthquake resistant design of buildings in the city of Babol (Iran). They showed that the numerical results obtained from one-dimensional soil behavior analysis and the experimental microtremor test results were in close agreement for underground alluvial conditions.

Fatahi *et al.* (2014) conducted a parametric numerical study on local site effects and soil-structure interaction (SSI). They concluded that the local site effects should be taken into account in nonlinear response analyzes, including SSI, to better understand the earthquake behavior of high-rise structures constructed on soft soil. Caruso *et al.* (2016) showed in their study on Eastern Sicily that the first important attempt to reliably obtain the geotechnical characteristics of the region was to accurately determine the shear wave velocity (Vs) of the ground profile. Also Castelli *et al.* (2016a) conducted a series of in-situ and laboratory dynamic and static tests to determine the ground geotechnical characteristics of the ancient city of Noto (Italy), located in a seismic region. 1D numerical analysis with the obtained data showed that the influences of the stratigraphic effects on the seismic response of Noto center area were shown to be possible to evaluate with these analyses. In some cases it was reported that seismic effects show significant amplifications.

Ferraro *et al.* (2016) conducted a detailed study to develop a geotechnical model for the city center of L'Aquila (Italy) by adopting the Down-Hole (DH), Seismic Dilatometer Marchetti (SDMT) and Multichannel Analysis of Surface Waves (MASW) test results. The soil amplification ratio based on one-dimensional equivalent soil behavior analysis was obtained to be higher than the respective value according to the Italian Building Code (NTC, 2008). In addition, the results obtained from the soil behavior analysis were compared to the damage observed during the earthquake in the region.

Sonmezer *et al.* (2019) performed one-dimensional equivalent linear site response analyses of the city center of Elazig, which is close to the Eastern Anatolian Fault Zone (EAFZ). They showed that the average surface acceleration spectrum obtained for the study area exceeded the proposed horizontal elastic design acceleration spectra of the Turkish Earthquake Code (TEC 2018) and Eurocode 8 (EC-8 2004). The results showed that multi-storey structures with high natural periods (1s) throughout the study area would be exposed to low Sa (spectral acceleration) values in zones with both low and high amplifications, while low-storey structures with short periods (0.2s) would be exposed to high Sa in certain regions.

The places struck by earthquakes in Turkey can be seen to be in the vicinity of the North Anatolian Fault Zone (NAFZ) and the East Anatolian Fault Zone (EAFZ). Erzincan-Karliova-Bingol triangle between NAFZ and EAFZ forms the eastern end of the Anatolian plate. Although EAFZ is seismically less active than NAFZ, historical evidence shows that it can, however, produce earthquakes up to M = 7.0 (Aktug *et al.* 2013). As shown in Fig. 1, Karliova-Bingol area between these two main fault systems is an area of intense deformations and constitutes the eastern boundary of the Anatolian plate. This area, where cross-fault systems developed between the two main fault zones, is the region with the greatest intensity of active faults in Turkey.

The aim of this study is to determine the regional distribution of ground magnification, soil dominant period, peak ground acceleration and 0.2-1 s period spectral acceleration values of the Karliova settlement area, which is under high earthquake risk. For this purpose, the soil behavior was tried to be characterized by using SHAKE 2000 (Ordonez 2012) software, which can perform one-dimensional equivalent linear (EL) analysis in the light of data obtained from seismic refraction, active source surface wave method (MASW) and standard penetration test (SPT).

2. Geology of the study area

Hinis metaophiolite and Bitlis metamorphites are located at the base of the outcrops in the study area. These rock units are overlain by Eocene-Lower Miocene formations with angular unconformity. These rock units are vertical and lateral transitive with each other and sometimes contain intercalations of lava and pyroclastic rocks. Lower Miocene and previous units are covered with angular unconformity by the formations of Middle Miocene, forming aged Bingol Mountain group. These units are overlain by formations of Upper Miocene Varto group with angular unconformity. The Varto group and older units are unconformably overlain by Lower Pliocene Hamurpet lava, Middle-Upper Pliocene, aged Yol formation and Quaternary units. Alluvials that cover a large area in the study area are generally composed of block, gravel, sand and clay size materials (Ilbank 2015).

3. Tectonics and seismicity

NAFZ is one of the active plate boundaries with the greatest population around the globe. This fault zone produced a series of destructive earthquakes during the 20th century. Therefore, great efforts have been made to evaluate its seismic behavior based on the historical and prehistoric seismic records (Barka 1996; Hubert-Ferrari *et al.* 2000). NAFZ constitutes one of Turkey's most important tectonic zones with its well-defined fault trace and seismic history. According to geodetic data, it has a 24-30mm yearly translation towards right (Reilinger *et al.* 1997). The cumulative displacement of the fault is estimated to range from 40 meters to several hundred meters.

The activity in the north-east of Turkey, initiated with the 1939 great Erzincan earthquake, continued westward with the 1942, 1943, 1944, 1951, 1957 and 1967 earthquakes (Toksoz *et al.* 1979; Barka 1996). Most of these strong and destructive earthquakes throughout NAFZ caused surface fractures. Two devastating earthquakes occurred on the western part of NAFZ. The first earthquake was the August 17th 1999 İzmit (Mw = 7.4) earthquake and the second one was the November 12th 1999 Düzce (Mw = 7.2) earthquake (Bürgmann *et al.* 2002). The NAFZ, which extends eastward along the Black Sea coast, consists of

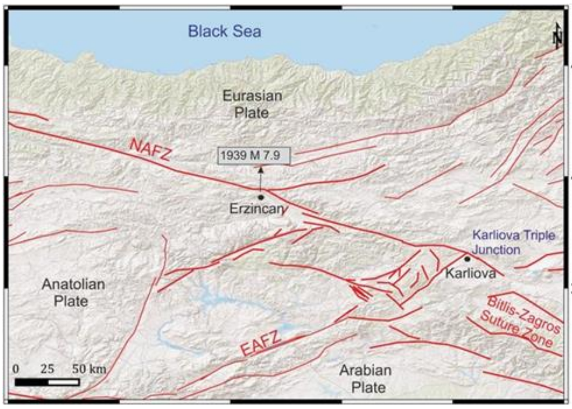

Fig. 1 Tectonics map of NAFZ and EAFZ (Bohnhoff 2016)

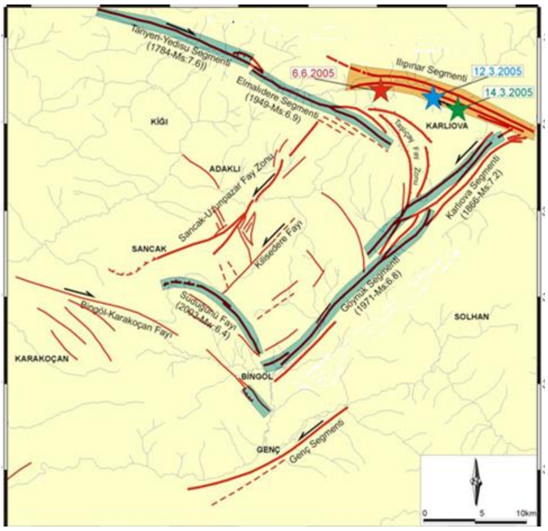

Fig. 2 Active fault zones map of the study area (Ozalp *et al.* 2005)

several parallel short faults, sometimes intersecting each other, and joins the left-oriented EAFZ in Karliova (Bozkurt 2001).

EAFZ is one of the active fault zones of Turkey. EAFZ extends a total distance of 580 km between Karliova and Antakya and plays an important role in the geodynamic evolution and seismicity of the region (Allen 1969; Saroglu *et al.* 1992; Ambrasseys 1989; Nalbant 2002). As shown in Figure 1, EAFZ forms the boundary between the Anatolian and Arabian plates and is defined as a left lateral strike-slip fault.

As shown in Fig. 2, Ilipinar and Elmalidere segments, which are located on NAFZ approximately 5 km away from Karliova, are 33 and 30 km long, respectively. An earthquake occurred in 1949 on the Elmalidere segment (Ms: 6.9) and surface faulting took place. The Tanyeri-Yedisu segment, which is 25 km away from Karliova further west, is 70 km long. The 1784 earthquake with a magnitude of Ms: 7.6 (Selim *et al.* 2005) originated from this segment. As shown in Figure 2, the EAFZ zone consists of two segments, namely the segment between Karliova and Goynuk and the one between Bingol and Karliova. The Karliova segment is 37 km long and is located at a distance of 5 km from Karliova. In this segment, Karliova (Mw: 5.7) earthquakes occurred on March 12th-14th, 2005. In 1866, it produced a major earthquake (Ms: 7.2), which resulted in surface faulting. The Goynuk segment, which is approximately 40 km long and is about 25 km away from Karliova, resulted in the 1971 Bingol earthquake of Ms: 6.8 (Kalafat 2006). In this study, dynamic soil properties of Karliova (Bingol) city center, which is very close to NAFZ and EAFZ intersection and which have high seismic hazard probability, were investigated. Karlıova is remarkable due to its increasing population and the presence many new buildings.

4. Seismic hazard analysis

Seismic hazard analyses are frequently used to determine the earthquake risk of a region. Seismic hazard analysis is defined as the numerical estimation of ground motion at local or regional scale. Seismic hazard can be analyzed by a deterministic method that takes into account specific earthquake scenarios or by a probabilistic method that takes into account the uncertainties associated with the probability, magnitude, impact and location of the earthquake (Kramer 1996; Chen 2002; Kramer 2009). In the probabilistic seismic hazard analysis (PSHA), all seismic sources that may affect the study area are taken into consideration and analyses are made according to the desired exceedance probability. As a result of these analyses, maps showing earthquake hazard of the study area can be prepared. In many studies, maps showing earthquake hazard were prepared based on seismic hazard analysis (Gulkan *et al.* 1993; Kijko and Graham 1998; Das *et al.* 2006; Kalkan *et al.* 2009).

In the literature, making a separate analysis for each source zone to determine the probabilistic seismic hazard is common. However, in this study, there are not enough earthquake records in the segments that create risk for the study area. Tanyeri-Yedisu and Ilıpınar segments on NAFZ and Göynük and Karlıova active fault segments on EAFZ, which are within 50 km distance, cause seismic risk to the study area. In addition, the earthquakes occurred in the study area generally took place in these segments. For all these reasons, PSHA was realized by taking into account the earthquakes of M_w> 4.5 occurring in a circular area with a radius of 50 km around Karliova. Earthquakes taken into consideration within the scope of the study are given in Table 1 and their locations are given in Figure 3.

Raw earthquake data obtained from different catalogs were compared in order to prevent duplication and one of the earthquakes with the same data was left in the database, while the others were removed. The magnitude values of all earthquakes occurred in Turkey in the last century, given at different scales (M_b: Body wave magnitude, M_L: Local magnitude, M_d: Time-dependent magnitude, M_s: Surface wave magnitude) and compiled by Deniz and Yücemen (2010) were converted into the moment magnitude (M_w) scale by using proper equations.

Researchers indicated that the Poisson model is a valid model for the formation of main shocks with major magnitudes and can be considered sufficient for engineering purposes (Kallberg 1969; Tunç *et al.* 2003). The Poisson model is based on the assumption that earthquakes occur independently from each other in terms of space and time. To ensure the independence condition required by the Poisson model, earthquake clusters should be determined and the leading and aftershocks (secondary earthquakes) must be removed from the seismic database (Yücemen 2011). Deniz (2006) determined the dimensions of time and space windows for secondary earthquakes within the above assumptions. Table 2 shows the dimensions of the time and distance windows obtained by the study conducted by Deniz (2006).

The probabilistic distribution of earthquake magnitude is obtained from repetition relations that give the relationship between the magnitude and occurrence of earthquakes. For this purpose, the linear size-to-number relationship, widely recommended by Gutenberg and Richter (1942, 1944, 1956) and Richter (1958) and given in Eq. 1, is widely used in the literature:

$$\log N = a - bM \tag{1}$$

where; N: The yearly number of earthquakes with a magnitude equal to M in a unit time, M: Earthquake magnitude, a and b: Regression coefficients

The probability of occurrence or exceedance of earthquakes of different magnitudes over a given time period can be estimated using Eqs. (2) and (3) according to the poisson distribution (P):

$$P(N \geq 1) = 1 - e^{-\lambda t} \tag{2}$$

$$\lambda = -\ln(1 - P)/t \tag{3}$$

where N is the parameter representing the number of earthquake occurrence, t is the time duration, λ is the average occurrence of the event.

When examining the effects of soil behavior exposed to seismic waves on structures, the most hazardous ground movement that will occur during the life of a structure should be determined. The design earthquake that causes such a ground motion is considered as an earthquake with a probability of exceedance of 10% during the 50-year service life of the structure or with a return period of 475 years (Yucemen 2011). This ground motion level has been used to design buildings in areas with high seismicity (Sitharam and Anbazhagan 2007). Using the seismic hazard analysis of Algermissen ve Perkins (1976); Cornell (1968) developed isosismic maps for bedrock-level horizontal peak ground acceleration and velocity based on 10 % probability of exceedance in 10 years. These maps were used for design response spectra in the 13th edition of the Bridge Design Specification of the American Association of State Highway and Transportation Officials (AASHTO 1983).

The number of occurrences and mass frequency values of earthquakes, determined by using the data obtained from earthquake catalogs, are shown in Table 2 for a circle with a radius of 50 km around the Karliova city center. The magnitude-occurrence number graph obtained by using these values is given in Fig. 4. According to PSHA, conducted for the city of Karliova by using the Poisson distribution and a probability of exceedance of 10 % in 50 years, the design earthquake magnitude was determined as

Table 1 Earthquakes used in the seismic hazard analysis

No	Date	Latitude	Longitude	Depth (km)	Magnitude (M_w)
1	25.05.2016	39.3482	40.9295	5	4
2	10.08.2005	39.35	41.09	15	4.1
3	20.07.2016	39.3573	40.5123	2.5	4.1
4	21.06.2016	39.4037	40.7345	5	4.1
5	15.03.2005	39.23	40.97	10	4.1
6	19.07.2016	39.3543	40.5177	1.3	4.2
7	21.07.2006	39.3612	40.8205	5	4.2
8	20.08.1966	39.3	40.82	70	4.3
9	01.03.1999	39.33	40.78	0	4.3
10	04.03.1997	39.33	40.98	12	4.3
11	23.06.1996	39.41	40.48	5	4.3
12	23.07.1969	38.9	41	169	4.4
13	27.10.2007	39.2982	40.7498	5	4.4
14	14.01.1900	39.4078	40.7807	5	4.4
15	01.02.2000	39.3	41.01	0	4.6
16	22.05.1971	39.23	40.61	50	4.7
17	23.03.2005	39.3877	40.7882	5	4.7
18	13.09.1966	39.17	40.85	46	4.8
19	20.08.1966	39.31	40.51	34	4.8
20	31.08.1965	39.3	41.2	33	4.8
21	15.12.1953	39.61	41.08	40	4.8
22	19.05.1948	39.43	41.31	20	4.8
23	23.08.1949	39.42	40.98	10	4.9
24	22.05.1971	39.08	40.63	41	5
25	01.10.1969	39.32	40.56	17	5
26	01.11.2006	39.4293	40.6477	5	5
27	02.07.2006	39.3412	40.9098	5	5
28	19.08.1966	39.41	41.3	62	5.2
29	27.08.1950	39.38	41.34	60	5.2
30	02.01.1950	39.3	41	30	5.2
31	13.04.1998	39.23	41.07	9	5.2
32	19.08.1966	39.33	41.25	39	5.3
33	07.07.1957	39.37	40.46	60	5.3
34	23.03.1953	39.37	41.28	50	5.3
35	13.10.1935	39.35	40.52	40	5.3
36	31.08.1965	39.36	40.79	11	5.4
37	05.03.1909	39.37	40.65	10	5.5
38	20.08.1966	39.42	40.98	14	5.6
39	09.12.1913	39.4	41.08	10	5.6
40	10.12.2005	39.3467	40.8557	5	5.7
41	25.08.2007	39.2588	41.0418	5	5.8
42	31.05.1946	39.29	41.21	60	5.9
43	14.03.2005	39.3475	40.8847	5	6.6

Table 2 Dimensions of distance and time windows to be used to differentiate between leading and aftershocks

Magnitude (M)	Distance (km)	Time (day)
4.5	35.5	42
5	44.5	83
5.5	52.5	155
6	63	290
6.5	79.4	510
7	100	790

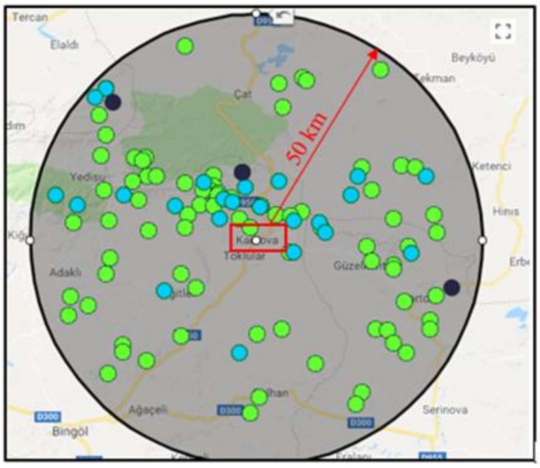

Fig. 3 Locations of earthquakes in the vicinity of the study area

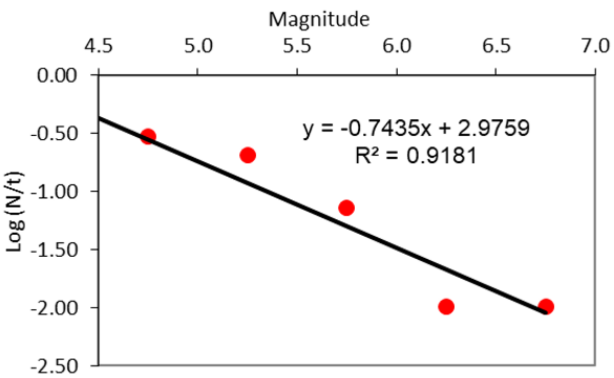

Fig. 4 Earthquake magnitude and number of occurrences relationship

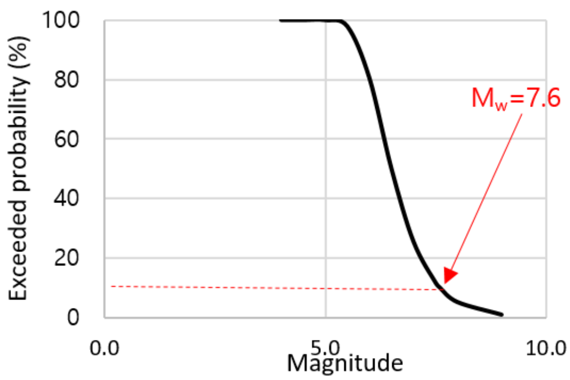

Fig. 5 Probability of occurrence-magnitude relationship according to poisson distribution for 50 years

M = 7.6 (Fig. 5).

Furthermore, Bohnhoff *et al.* (2016) reported earthquake magnitudes ranging between M=7.4 in the west and M=7.9 in the east based on the seismic catalog data of the entire NAFZ, covering a period of 2300 years. They stated that the largest earthquakes (M = 7.8-8.0) could be observed along the eastern segments of the NAFZ. Taking into account all these evaluations, the magnitude of the design earthquake in Karliova was considered as M_w=7.6.

Structures in earthquake zones are subjected to different levels of earthquake effects. Ground motion parameters required for the earthquake-resistant design of structures can be determined by attenuation relationships (Kramer 1996). Ground motion attenuation relationships have been obtained by various researchers around the globe (Boore *et al.* 2013; Akkar and Bommer 2007; Ambraseys and Bommer 1991; Campbell 1989; Joyner and Boore 1981). These relationships take into account the geological conditions of the site, earthquake source mechanism and source distance. They are developed by regression analysis using recorded strong ground motion data (Akın 2009).

Attenuation relations, developed using strong motion records in Turkey, are also available in the literature (Ozbey *et al.*2004). Most are based on the data obtained in 1999 Kocaeli earthquake in the Marmara region. Nevertheless, instead of utilizing the weighted local attenuation relationship of the 1999 Kocaeli earthquake,the target spectrum of the present study was developed by using the new-generation attenuation relationships proposed by Abrahamson *et al.* (2013) (ASK 2013), Boore *et al.* (2013) (BSSA 2013) and Campbell and Bozorgnia (2013) (CB 2013) within the project "Next Generation Attenuation WEST2 (NGA-West2 2013)"of the Pacific Earthquake Engineering Research Center (PEER) (PEER 2017). These relationships are based on a wide database consisting of earthquake records from Turkey and different parts of the globe.

The fault rupture processive local soil conditions are known to be of great importance for near- and far-field earthquakes. Seismic sources in and around the study area can be denoted as close and distant ones. As shown in Fig. 2, the Karliova study area is under the influence of the nearby fault segments (Ilipınar, Elmalidere and Karliova) at a distance of 5 km as well as the distant fault segments (Goynuk and Tanyeri-Yedisu) at a distance of 25 km. For this reason, using the abovementioned attenuation relationships target spectra were obtained from the PEER database for both the near-field and far-field earthquake scenarios for the bedrock level and these spectra are given Figs. 6(a) and 6(b) respectively.

The site response analyses start with obtaining earthquake records scaled to the target spectrum (Sun *et al.* 1988; Yucemen 2011). The quantitative measure used for evaluating the agreement of a record with the target spectrum is the Mean Square Error (MSE), which is defined as the natural logarithmic difference between the spectral acceleration values in the target and recorded response spectra and calculated from Eq. 4 (PEER 2017).

$$MSE = \frac{\sum_i w(T_i\{ln[SA^{target}(T_i)] - ln[f \times SA^{recorded}(T_i)]\}^2}{\sum_i w(T_i)} \quad (4)$$

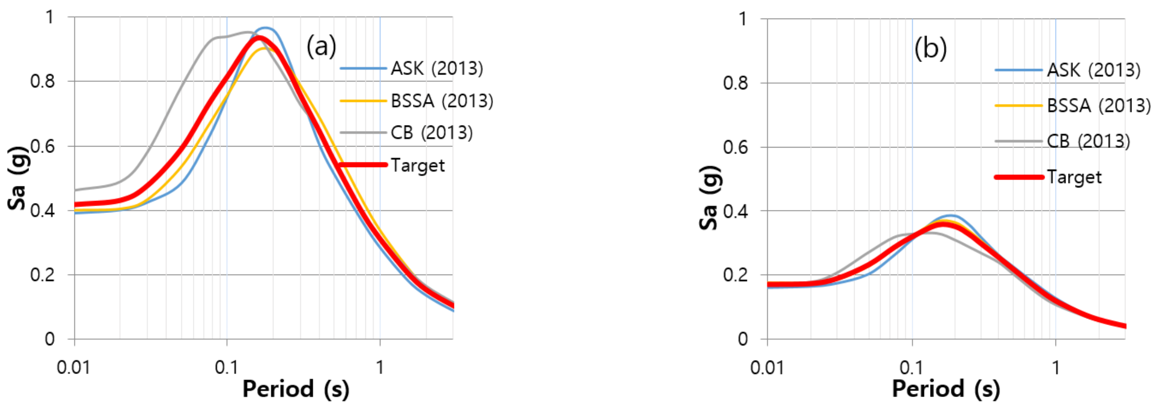

(a) Near-field earthquake scenario (b) Far-field earthquake scenario

Fig. 6 Target spectrum of the bedrock level

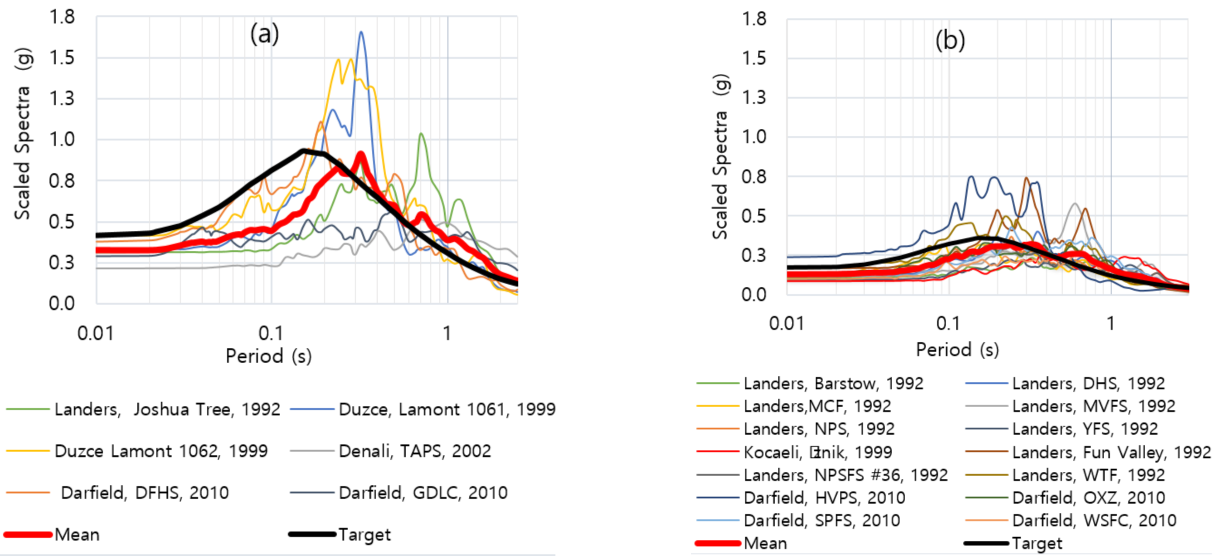

(a) Near-field earthquake scenario (b) Far-field earthquake scenario

Fig. 7 Bedrock acceleration spectra of earthquake records scaled to the target spectrum

where; MSE: Mean square error, SA^{target}: Target acceleration response spectrum, $SA^{recorded}$: Acceleration spectrum of the used record, w: Weight function (insimple casew (Ti) =1), f : Scale factor

The scale factor (f) allows the generation of scaled recordings that best match the shape of the target spectrum in the user-defined period interval (PEER 2017). The scale factor (f) is calculated using Eq. (5)

$$lnf = \frac{\sum_i w(T_i) ln(SA^{target}(T_i)/SA^{recorded}(T_i))}{\sum_i w(T_i)} \tag{5}$$

In this study, 6 earthquake records for the far-field and 14 records for near-field earthquake scenario, scaled to the target spectrum, were selected from the PEER database as the bedrock level earthquake motion. When determining earthquake records from the PEER database, the distance of the study area to the fault was taken as 5 km for near-field and 25 km for far-field earthquake records. The shear wave velocity at the upper 30 m was calculated using Eq. 6 using the data obtained from the seismic refraction tests at 30 locations and it was found to be in the range of 166-588 m/s.

$$V_{s30} = \frac{30}{\left(\frac{h}{V_{s1}} + \frac{(30-h)}{V_{s2}}\right)} \tag{6}$$

where; V_{s30}: Shear wave velocity at 30 m, h: Thickness of the first layer (m), V_{s1}: Shear wave velocity of the 1st layer (m/s),V_{s2}: Shear wave velocity of the 2nd layer (m/s)

In addition, the earthquake magnitude determined from PSHA was considered as 7.6. Scaling of the determined earthquake records to the target spectrum was performed using the scaling tool on the simulation platform of the PEER website. The acceleration spectra of the determined near-field earthquake records are given in Fig. 7(a), while the spectra for the far-field records are shown in Fig. 7(b).

5. Geotechnical site conditions

In the study area, 47 geotechnical borings having a depth of 5.00-15.00 m were carried out at a depth of 454 m from the surface in order to determine the dynamic behavior characteristics of the soils. Standard Penetration Test (SPT) was performed in the borings and 213 disturbed samples

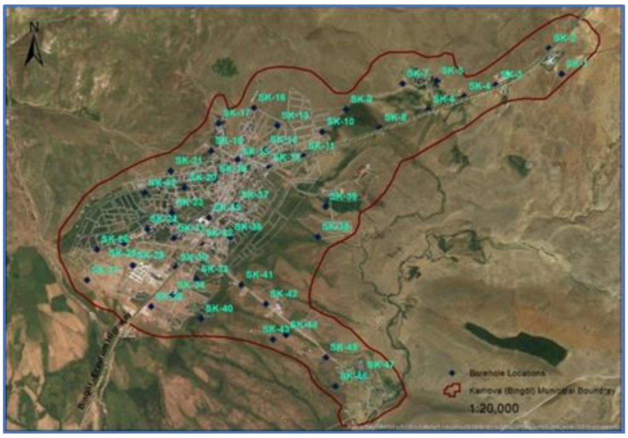

Fig. 8 Locations of the borings in the study area

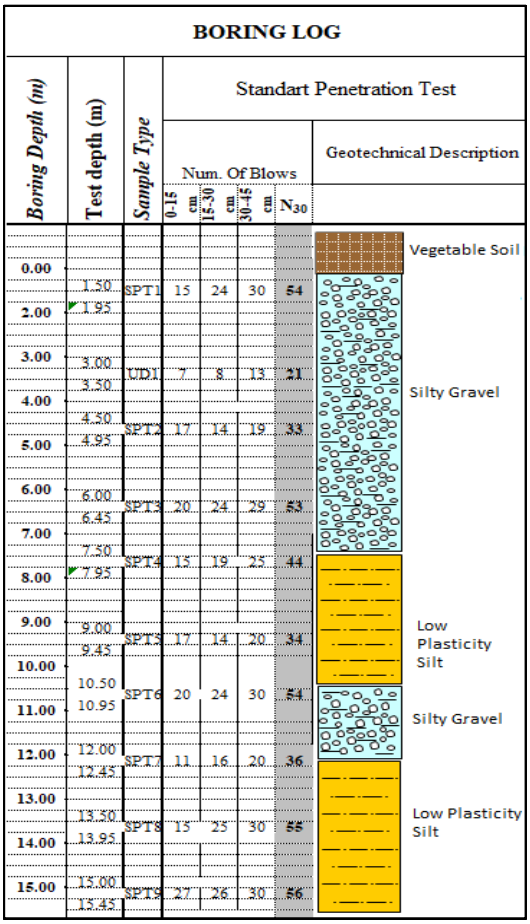

Fig. 9 An example boring log and the corresponding SPT values

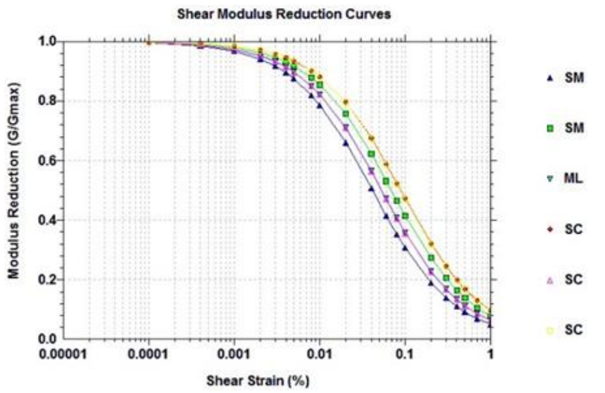

Fig. 10 Shear modulus reduction curves for typical soil profile

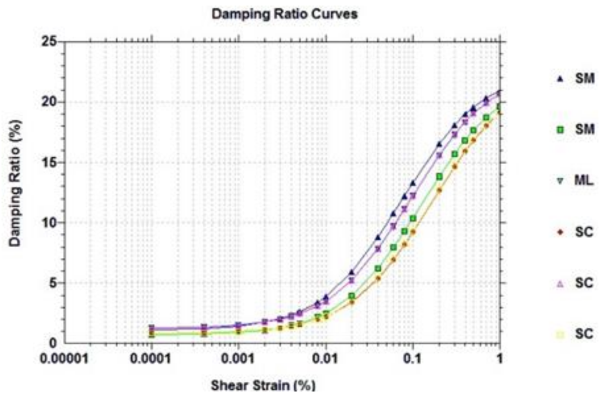

Fig. 11 Damping ratio curves for the typical soil profile

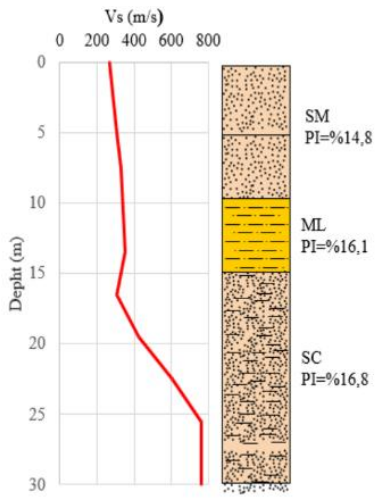

Fig. 12 Typical soil profile for Karliova

and 18 undisturbed samples (UD) were taken. In addition, 30 Multichannel Analysis of Surface Waves (MASW) and 30 seismic refraction tests were performed in the study area. The locations of the borings in the study area are given in Figure 8 and an example boring log is depicted in Fig. 9. Shear wave velocity (Vs) is often used to characterize soil behavior in site response analyses (Akin *et al.* 2013, Eskişar *et al.* 2014, Kolat *et al.* 2012, Selçuk and Çiftçi 2007, Sonmezer *et al.* 2015, Ulusay *et al.* 2004). When Vs measurements are not taken in field studies, Vs and/or maximum shear modulus (Gmax)can be estimated from SPT, plasticity index (PI) and grain size distribution through various correlations (Vucetic and Dobry 1991; Kramer 1996). Various researchers developed and reported equations which provide the relationship between the SPT impact number and Vs (Dikmen 2009, Hanumantharao and Ramana 2008, Iyisan 1996, Seed and Idriss 1981). For Karlıova, the correlation developed by Iyisan (1996) which is valid for all soil types in order to determine shear wave velocity from SPT values at each bore point, was preferred. Records from strong ground motion seismographs placed vertically at different depths and research showed that the effect of the soil and rock layers within the upper 30 m from the surface on the dynamic soil properties is rather important (Borcherdt 1994). In cases where the drilling depths do not reach the engineering bedrock, the soil parameters at the depth of 30 m will be sufficient to represent the ground (Midorikawa 1987, Borcherdt 1994) and have been used in many studies (Finn and Ventura 1995, Ansal 2004, 2005). In addition, in the NEHRP 2003 (NEHRP 2003) specification and the European seismic regulation (EC8 2004) the soil classification is based on the average shear wave velocity at the upper 30 m. In this study, drilling depths did not reach the engineering bedrock, so Shake2000 software (Ordonez 2012) was used by taking the drilling depth as 30 m. In their experimental study, Hardin and Drnevich (1972) determined that Vs has an exponential variation (a power of 0.25) from the surface to the bedrock in terms of stress. Robertson *et al.* (1992) normalized Vs with respect to the stress. In some boring wells of the present research, where Vs could not be determined from 20 to 30 m, the equation of Robertson *et al.* (1992) was used, which is given Eq. (7):

$$V_{s1} = V_s(P_a/\sigma_v')^{0,25} \tag{7}$$

where; P_a is the atmospheric pressure (100 kPa), V_s the shear wave velocity, V_{s1} the normalized shear wave velocity and σ_v' the effective vertical pressure.

The shear wave velocity at any depth can be determined from the seismic refraction test, the MASW test, or the empirical formulas based on SPT. For example, on a ground with a unit volume weight of 19 kN/m^3, if the shear wave velocity at 20 m is determined to be 300 m/s from the mentioned tests, the shear wave at 25 m according to Eq. (7) is as follows:

$$300\ m/s = V_s \times \left(\frac{100}{19\times 25}\right)^{0.25} \quad V_s = 442.9 \text{ m/s}$$

calculated.

Here; The shear wave velocity (300 m / s) at 20 m obtained from the test is already the actual value that contains the depth effects. The shear wave velocity (Vs) at 25. m is calculated as 442.9 m / s depending on the increase in depth and the effective stress.

Stress-deformation properties of soils are defined by considering the change of shear modulus and damping ratio with the level of shear deformation (Bardet *et al.* 2000). Shear modulus and damping ratio of soils are widely accepted as a function of shear strain under repeated loads. The change of soil stiffness by deformation is determined from the damping ratio (D) and shear modulus reduction (G/Gmax) curves. G/Gmax and D curves are the fundamental parameters of site response analyses performed using nonlinear and equivalent linear techniques (Hanumantharao and Ramana 2008). G/Gmax and D curves for different types of soils have been studied by several researchers in the literature (Seed *et al.* 1986, Vucetic and Dobry 1988, Sun *et al.* 1988, Darendeli 2001, Capilleri *et al.* 2014, Castelli *et al.* 2016b). G/Gmax and D curves,which were proposed by Darendeli (2001) and consider the effect of the surrounding pressure and plasticity index simultaneously, were used in the site response analyzes of the present study. The G/Gmax and D curves used in the typical soil profile are given in Figs. 10 and 11, respectively. In this study, the typical soil profile (Fig. 12) was obtained for the study area by taking the average of the Vs values and PI values for all boreholes and by determining the main types of soil. All boring logs were examined while determining the typical soil profile. In these logs, the average gravel content of the unit between 0-10 m was obtained as 21.6 %, the sand content 33.3 %, the fine grain ratio (silt + clay) 45.1% and PI = 14.8 %. The average gravel content of the unit between 10-15 m, on the other hand was determined as 18 %, the sand content 18.9%, the fine grain ratio (silt + clay) as 63.1% and PI = 16.1 %. The seismic fracture and MASW tests showed that the soil between 15 and 30 m depth consists mainly of alluvium. In addition, the mean Vs values obtained from the drilling logs varied between 269-309 m/s at depths 0-15 m and 309-760 m/s at depths 15-30 m.Considering the above data and Vs values, the study area is composed of ZC (360-760 m/s) and ZD (180-360 m/s) types of soil according to Turkish Earthquake Code (TEC 2018) B (360-800 m/s) and C (180-360 m/s) classes of soil according to Eurocode 8 (EC-8 2004).

6. Dynamic site response analyses

In areas subjected to earthquake hazards, different soil classes transmit cyclic loads, such as earthquake loads, to the superstructures differently. Changes in the soil cross-section can lead to amplification or damping of these repetitive loads, depending on the frequency characteristics. These amplifications and dampings cause different acceleration – time values on the ground surface and therefore different response spectra (Unutmaz *et al.* 2011).

Shake2000 (Ordonez 2012) software was used to determine the dynamic soil properties and surface response spectra of the study area. This software calculates the response in a visco-elastic homogeneous system, which extends horizontally to infinity, affected by vertically propagating shear waves. This program is based on the repetitive solution of wave equations adapted for the use for short-duration motions by means of the Fourier transform algorithm.

Within the scope of the study, site response analyzes were performed in Shake2000 (Ordonez 2012) software using unit weight (γn), shear wave velocity (Vs) and shear modulus reduction (G/Gmax) and damping ratio (D) curves on a typical ground profile and the ground profile of each borehole. The frequency content of the possible earthquake in the study area could not be known exactly. Therefore, instead of using a single earthquake record with known frequency content in site response analyzes, 14 different earthquake records for the far-field earthquake scenario scaled to the target spectrum and 6 different earthquake records for the near-field earthquake scenario were used in the analyses.

The acceleration spectra of all earthquake records and their average acceleration spectrum were obtained by using 6 earthquake records for the near-field earthquake scenario and 6 records for the far-field earthquake scenario on the

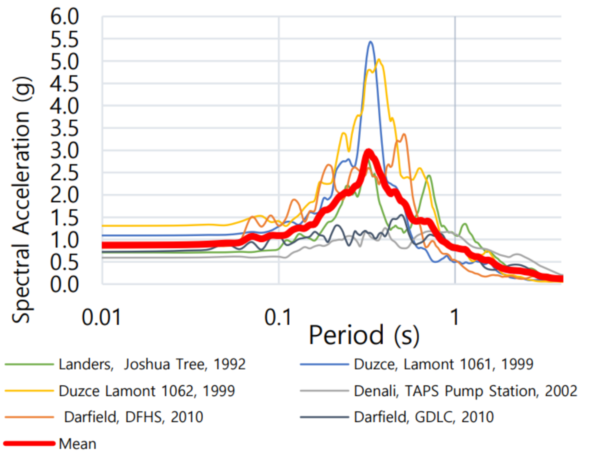

Fig. 13 Acceleration spectra of the scaled records and mean acceleration spectrum from the analyses on typical gorund profile and near-field earthquake scenario

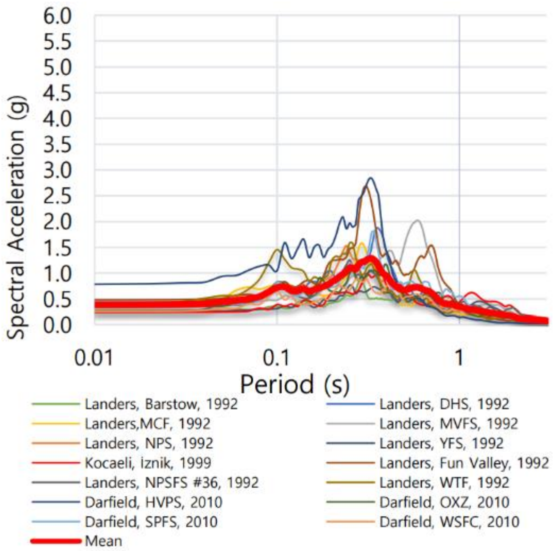

Fig. 14 Acceleration spectra of the scaled records and mean acceleration spectrum from the analyses on typical gorund profile and far-field earthquake scenario

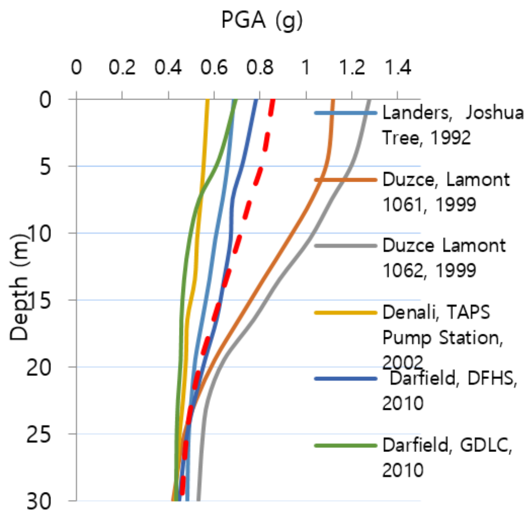

Fig. 15 PGA of the scaled records and mean PGA from the analyses on typical gorund profile and near-field earthquake scenario

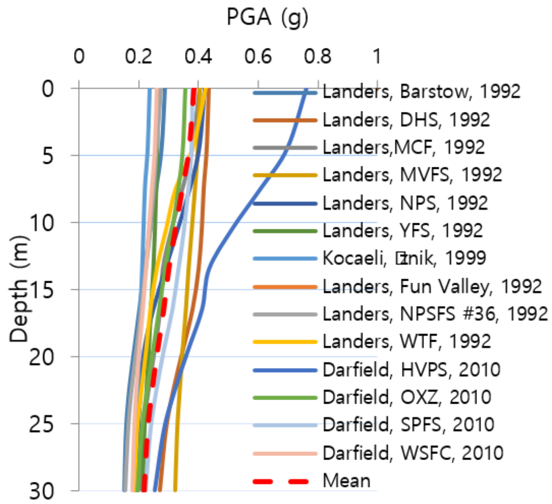

Fig. 16 PGA of the scaled records and mean PGA from the analyses on typical gorund profile and far-field earthquake scenario

typical ground profile and they are given in Figs. 13 and 14, respectively.

The maximum spectral acceleration changes between 1.25g and 5.4g for the far-field earthquake scenario with an average value of 2.95g, whereas between 0.85 g and 2.83g with an average of 1.28g for the far-field earthquake.

In addition, the transfer function between the bottom layers of the soil profile and surface and graph of the near-field peak ground acceleration (PGA), depending on the depth, is given in Fig. 15, while the PGA graph forthe far-field earthquake is shown in Fig. 16. Near-field PGA values range from 0.57 to 1.27 g, with an average of 0.85 g. The far-field PGA values range from 0.23 to 0.76 g, with an average of 0.38 g.

Most earthquake regulations define the strong ground motion that the engineer should take into account in the structural design through the concept of design spectrum (Akkar and Gulkan 2002). The near-field and far-field mean acceleration spectra obtained from the analyses on the typical soil profile, which is an important indicator for the study area soil, are compared to the spectra corresponding to the ZC and ZD type of soils in Turkish Earthquake Code (TEC 2018) and the ones for the B and C class soils according to Eurocode 8 (EC-8 2004). This comparison is shown in Figs. 17(a)-17(d).

The predominant period of the dominant motion of near-field earthquakes is relatively less than the dominant period of far-field earthquakes at the bedrock level of the same region. Near-field earthquakes produce seismic waves with high frequency harmonics, while far-field earthquakes may have low frequency harmonics, and the predominant period of such seismic movements may be close to or equal to the ground dominant period of deep alluvial soils. In this case, resonance conditions may develop in multi-storey structures in alluvial zones and may cause significant damage to such structures.

The results obtained from the analyses within the scope of the study clearly show that the average response spectrum obtained for the near-field earthquake scenario is

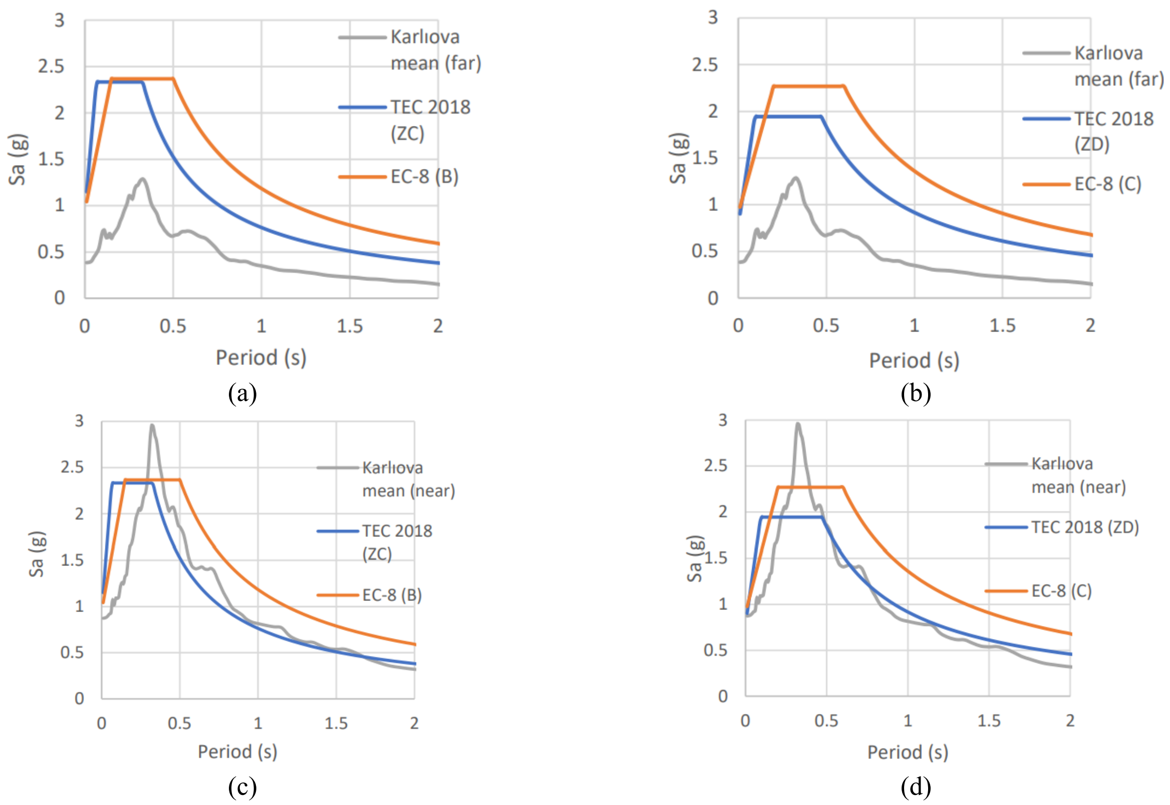

Fig. 17 (a) Average spectrum, TEC 2018 (ZC), EC-8 (B) spectra for the far-field, (b) Average spectrum, TEC 2018 (ZD), EC-8 (C) spectra for the far-field, (c) Average spectrum, TEC 2018 (ZC), EC-8 (B) spectra for the near-field and (d) Average spectrum, TEC 2018 (ZD), EC-8 (C) spectra for the near-field

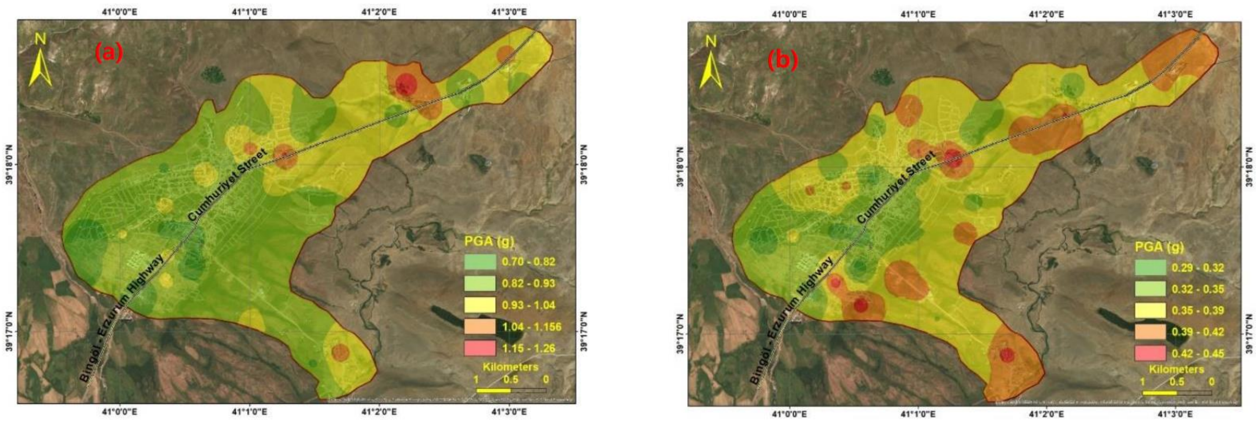

(a) Near-field earthquake scenario (b) Far-field earthquake scenario

Fig. 18 PGA map for Karliova

above the ZC and ZD design spectra of Turkish Earthquake Code (TEC 2018) whereas it remains below the B and C design spectra of the Eurocode 8 (EC-8 2004). except the peak level. The average response spectrum obtained for the far-field earthquake scenario is below both the ZC and ZD design spectra prescribed for Turkish Earthquake Code (TEC 2018) and B and C design spectra for Eurocode 8 (EC-8 2004).

The Karliova mean spectrum obtained for the near-field earthquake scenario and for the typical soil profile exceeds the Turkish Earthquake Code (TEC 2018) ZC design spectrum in periods beyond 0.3 sec, while it exceeds the ZD spectrum between 0.15-0.49 s. The mean spectrum surpasses the Eurocode 8 (EC-8 2004). (B) spectrum and the EC-8 (C) spectrum in narrower period ranges of 0.3-0.4 s and 0.3-0.42 s, respectively. The results here clearly show that the design spectrum of the Eurocode 8 (EC-8 2004). represents the soil in the study area than the design spectrum of Turkish Earthquake Code (TEC 2018).

Considering this situation in terms of the existing structures in the study area, the natural periods of many reinforced concrete buildings in Karliova falls between these mentioned periods. In a possible near-field earthquake scenario that will occur in the study area, the buildings with

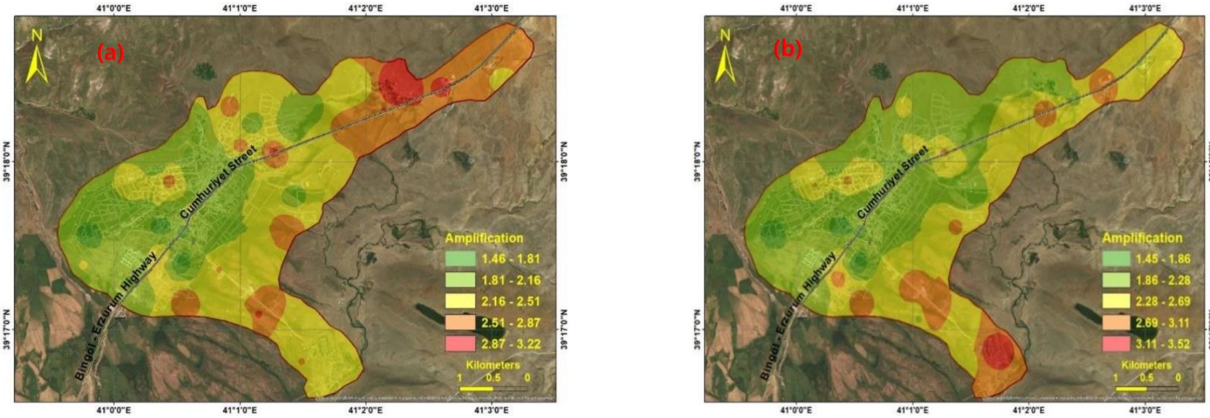

(a) Near-field earthquake scenario (b) Far-field earthquake scenario

Fig. 19 Amplification map for Karliova

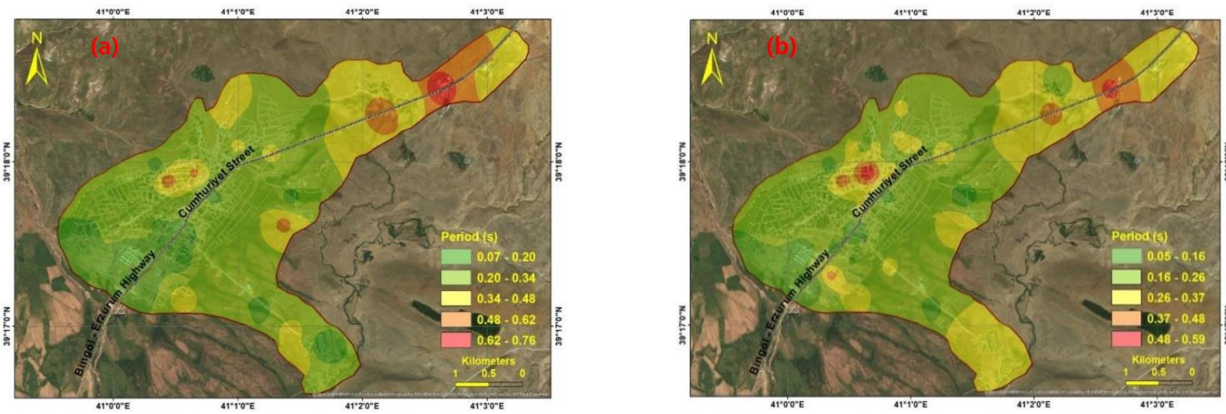

(a) Near-field earthquake scenario (b) Far-field earthquake scenario

Fig. 20 Predominant site period map for Karliova

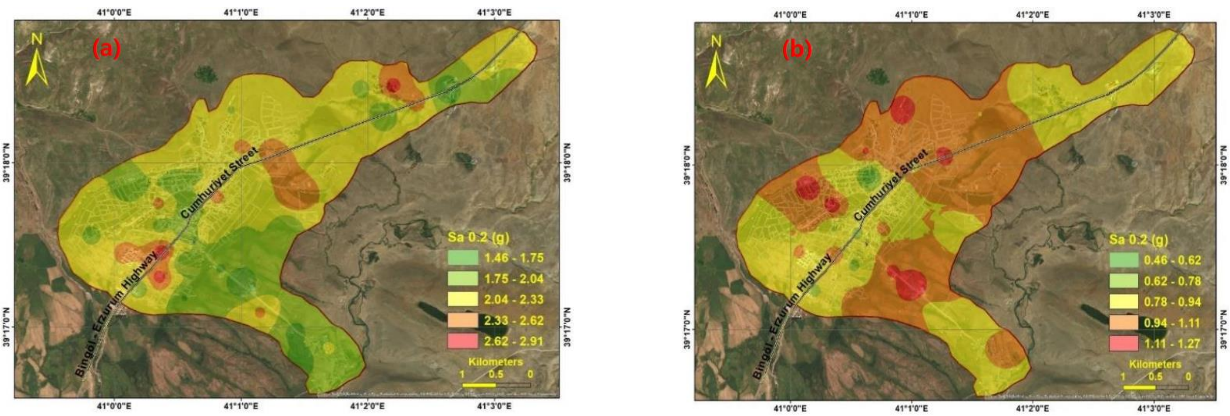

(a) Near-field earthquake scenario (b) Far-field earthquake scenario

Fig. 21 0.2-s period Sa map for Karliova

periods between these periods will be exposed to higher accelerations. The regional distribution of this situation, which varies depending on soil properties, is shown in the maps given at the end of this section. As in the typical soil profile, spectral accelerations that may exceed the code design spectra may develop in some regions of the study area. This study reveals that local soil conditions should be taken into consideration in earthquake resistant building design.

Within the scope of the study, one-dimensional equivalent linear site response analyzes were performed for both near- and far-field earthquakes in Shake2000 (Ordonez 2012) software, using the data from 47 boreholes throughout the field. As in the typical soil profile, 6 earthquake records for the near-field earthquake scenario and 14 for the far-field scenario were used for the analyses of each boring location.

The average values of the data obtained from the

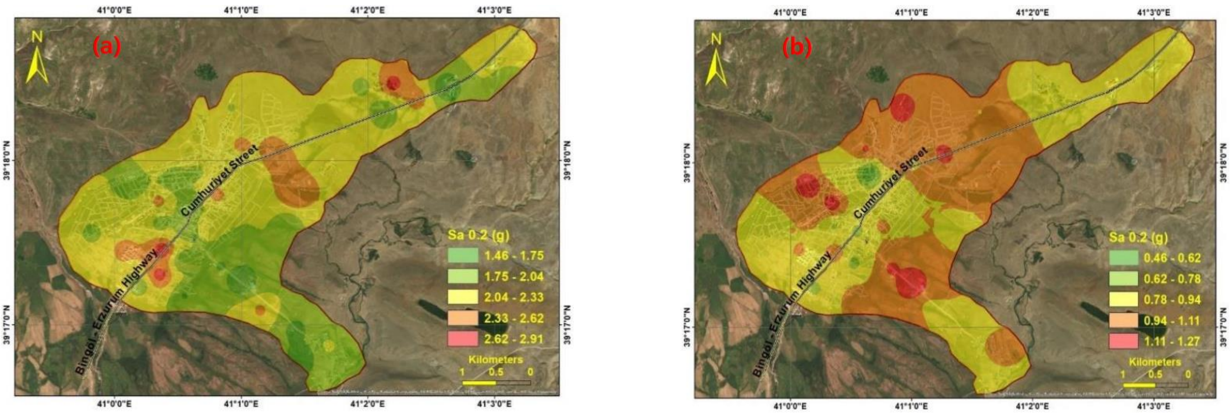

(a) Near-field earthquake scenario (b) Far-field earthquake scenario

Fig. 22 1-s period Sa map for Karliova

analysis for each earthquake record were used to determine the dynamic soil properties of that location. Then, using these data in ARCGIS software (ESRI 2013), PGA, ground amplification ratio, ground dominant period and 0.2 and 1-s spectral acceleration maps of the study area were prepared for both near-field and far-field earthquake scenarios and these maps are shown in Figs. 18-22.

The maps obtained from site response analyses can give us an idea of which residential areas are appropriate for multi-storey construction and which are appropriate for low-storey construction by presenting spectral acceleration values in 0.2-1 s periods, PGA and ground dominant period values especially as a result of soil amplification in the region during a possible earthquake. The mapping using the maximum value of the surface spectral acceleration, obtained from the site response analyses, is not very useful as it does not show the periods corresponding to different accelerations. However, mapping according to 0.2 s (short period) and 1.0 s (long period) values is more useful and more enlightening in defining resonance event (Sonmezer *et al.* 2018).

The PGA values determined from the site response analyses of the study area and given in Figure 18 vary between 0.70-1.26 g for the near-field earthquake scenario. High PGA values are observed in a small portion to the north of the study area, while it is 0.70-0.93 g in a major portion of the study area. With the exception of some local regions, PGA values vary between 0.29g and 0.45gwith an average of 0.35 g for the far-field earthquake scenario. Soil amplification rates, given in Fig. 19, vary between 1.45 and 3.52 for both near- and far-field earthquake scenarios. High amplification values are observed in the region to the north of the study area for the near-field earthquake scenario, while high.

Amplification values are observed in the southern regions for the far-field earthquake scenario.

In Fig. 20, the predominant site period of the soil in the study area ranges between 0.07-0.76 s according to the near-field earthquake scenario. The high period values of 0.6-0.7 s are observed in the north of the study area, while the period commonly ranges between 0.2 and 0.3 s in the entire study area. According to the far-field earthquake scenario, the predominant site period in the study area varies between 0.05-0.59 s and is generally between 0.05-0.26 s. In Fig. 21, for the near-field earthquake scenario, spectral accelerations for a period of 0.2 s (short period) vary between 1.46-2.91 g, while they range between 0.46 and 1.27g station for the far-field earthquake scenario. The spectral accelerations for a period of 1.0 s (long period), given in Fig. 22, vary between 0.64 and 1.39 g, while they change between 0.31 and 0.46 g for the far-field earthquake scenario. When all these data are evaluated, medium-level amplification ratios (2.5-3) are observed in the northern regions of the study area for the near-field earthquake scenario and in the southern regions of the study area for the far-field earthquake scenario. Regarding the overall study area, amplification ratios for both near and far-field earthquake scenarios are as low as 1.5-2. However, the periods corresponding to the amplification ratio values and the spectral acceleration (Sa) values at these amplification levels are as important as the amplification ratios themselves. In this context, in the northern regions where the amplification ratios are high for the near-field earthquake scenario, the predominant site period is in the order of 0.49-0.76 s, while it is in the order of 0.2-0.3 s for the entire study area. For the far-field earthquake scenario, the predominant site period in the southern regions is between 0.26-0.4 s. The predominant site period values in the study area can be said to be generally low (0.2-0.4 s). When the Sa values corresponding to the 0.2 s and 1 s periods are examined, the Sa values for the near-field earthquake scenario is in the order of 1.75-2.33 g, except for some small regions for short period, while the Sa ranges between 0.64-0.94 g for small localities in the north and middle of the region for long period. For the far-field earthquake scenario, the Sa values for the period of 0.2 s vary from 0.78 to 1.27 g, while the Sa values for the 1 s period are generally in the order of 0.3-0.4 g, except for some small zones.

In the study area, the Sa values corresponding to 0.2 s period were seen to be higher than the respective values corresponding to 1 s period. When this finding is evaluated in terms of the structures to be constructed in the study area, the low-rise structures (2-4 floors) in the study area can be found to be exposed to high Sa values while the multi-storey structures (8-10 floors) to lower Sa values. These results are important and should be taken into consideration in order to be affected as little as possible from the future earthquakes in both urban transformation areas and new construction areas

5. Conclusions

This study reveals the necessity of considering local soil conditions for earthquake-resistant building design in Karliova (Bingol) city center, located at the intersection of the NAFZ and EAFZ active fault zones. For this purpose, the seismic hazard analysis was performed first and the design earthquake magnitude in the study area was determined as Mw = 7.6. Taking into account this magnitude of earthquake, the target spectrum was established for both the near- and far-field target

earthquake scenarios and for the bedrock level by using the new-generation reduction relationships. One-dimensional equivalent linear site response analyses were performed for each borehole using the earthquake records, scaled to this target spectrum. Soil amplification ratio, ground dominant period, PGA and Sa contour maps with T = 0.2 and T = 1.0 s periods were obtained from the analyses. The results of this study show the need to develop contour maps of ground parameters for determining the local surface spectra and to reduce the negative effects of earthquakes. Other important conclusions and findings of the present study are summarized below:

• Using the data on previous earthquakes in the study area, the earthquake magnitude with 10% possibility of exceedance in 50 years was determined to be Mw=7.6 for the study area based on probabilistic seismic hazard analysis.

• The average surface acceleration spectrum obtained for the near-field earthquake scenario and from the typical ground profile was shown to exceed the Turkish Earthquake Code (TEC 2018) design spectrum for the ZC class of soil for natural periods above 0.3 s, while it exceeds the design spectrum for the ZD soil class for period values between 0.15 and 0.49 seconds. The average surface acceleration spectrum was determined to exceed the Eurocode 8 design spectra for the B and C soil types in a narrower range of periods, i.e. 0.3-0.4 s and 0.3-0.42 s, respectively. The average surface spectra obtained for the far-field earthquake scenario, on the other hand, do not exceed the design spectra of the two codes. Accordingly, the design spectrum of the EC-8 (2004) represents the ground in the study area better than the design spectrum of the TEC (2018) regulation.

• The PGA values for the near-field earthquake scenario, determined from the soil response analyses of the study area, range between 0.70 g and 1.26 g. High PGA values are observed in a small region in the north of the study area, while the PGA values are in the range of 0.70-0.93 g in most of the study area. According to the far-field earthquake scenario, PGA values range between 0.29g and 0.45 g. With the exception of certain local regions, PGA is in the order of 0.35g.

• According to the data obtained from the soil response analysis, the predominant site period in the study area for the near-field earthquake scenario varies between 0.07-0.76 s. The high period values of 0.6-0.7 s are observed in the north of the study area and generally range between 0.2-0.3 s. According to the far-field earthquake scenario, the predominant site period in the study area varies between 0.05-0.59 s and is generally between 0.05-0.26 s.

• In the study area, the spectral acceleration (Sa) values for 0.2-s period are in the range of 1.75-2.33 g for the near-field earthquake scenario with the exception of certain local regions. Yet, the Sa values for 1-s period are generally in the order of 0.64-0.94 g with the exception of two small local regions in the north and middle of the area. For the far-field earthquake scenario, however, the Sa value for 0.2-s period changes between 0.78g and 1.27g and the respective value for 1-s period changes in the range of 0.3-0.4 g except certain small localities.

• In the study area, the spectral acceleration (Sa) values for 0.2-s period are higher while the respective values for the 1-s period are relatively lower for both the near-field and far-field earthquake scenarios. Accordingly, the low-rise buildings with low modal vibration durations in the study area are expected to be exposed to high Sa and high-rise buildings with high modal vibration durations to lower Sa values.

Acknowledgments

We would like to express our gratitude to Dulkadiroglu Geotechnical and Mining Limited Company for their help in obtaining the data in the study area.

References

Abrahamson, N.A., Silva, W.J. and Kamai, R. (2013), "Update of the AS08 ground-motion prediction equations based on the NGAWest2 data set", Pacific Earthquake Engineering Research Center (PEER), University of California, Berkeley, California, U.S.A.

Akın, M. (2009), "Seismic microzonation of Erbaa (Tokat-Turkey) located along eastern segment of the North Anatolian Fault Zone (NAFZ)", Ph.D. Dissertation, Middle East Technical University, Ankara, Turkey.

Akın, M.K., Topal, T. and Kramer, S.L. (2013) "A newly developed seismic microzonation model of Erbaa (Tokat, Turkey) located on seismically active eastern segment of the North Anatolian Fault Zone (NAFZ)", *Nat. Hazards* **65**(3), 1411-1442. https://doi.org/10.1007/s11069-012-0420-1.

Akkar, S. and Bommer, J.J. (2007), "Empirical prediction equations for peak ground velocity derived from strong motion records from Europe and the Middle East", *Bull. Seismol. Soc. Amer.*, **97**(2), 511-530. https://doi.org/10.1785/0120060141.

Akkar, S. and Gulkan, P. (2002), "Tasarım spektrumlarının performansa dayalı deprem mühendisliği (PDDM) ve yakın mesafe depremler yönünden incelenmesi", *Proceedings of the Uluslararası Yapı ve Deprem Mühendisliği Sempozyumu*, (ECAS2002), Ankara, Turkey.

Aktug, B., Dikmen, U., Dogru, A., Ozener, H. (2013), "Seismicity and strain accumulation around Karliova Triple Junction (Turkey)", *J. Geodyn.*, **67,** 21-29. https://doi.org/10.1016/j.jog.2012.04.008.

Algermissen, S.T. and Perkins, D.M. (1976), "A probabilistic estimate of maximum acceleration in rock in the contiguous United States", Report, U.S. Geological Survey, U.S.A.

Allen, C.R. (1969), "Active faulting in northern Turkey", Division of Geological Sciences, California Institute of Technology, Pasadena, California, U.S.A.

Ambraseys, N.N. and Bommer J.J. (1991), "The attenuation of ground accelerations in Europe", *Earthq. Eng. Struct. Dyn.*, **20**, 1179-1202. https://doi.org/10.1002/eqe.4290201207.

Ambraseys, N.N. (1989), "Temporary Seismic Quiescence: SE Turkey", *Geophys. J.*, **96**(2), 311-331. https://doi.org/10.1111/j.1365-246X.1989.tb04453.x.

Ansal, A., Biro, Y., Erken, A. and Gülerce, Ü. (2004), *Seismic Microzonation: A Case Study*, in *Recent Advances in Earthquake Geotechnical Engineering and Microzonation*, Springer Netherlands, Dordrecht, 253-266. https://doi.org/10.1007/1-4020-2528-9_9.

Ansal, A., Özaydın, K., Erdik, M., Yıldırım, H., Kılıç,, H., Adatepe, Ş., Özener, P.T., Tonaroğlu, M., Şeşetyan, K. and Demircioğlu, M. (2005), "Seismic microzonation for urban planning and vulnerability assessment", *Proceedings of the International Symposium of Earthquake Engineering (ISEE2005)*, Awaji Island, Kobe, Japan.

AASHTO, (1983), *Standart Specifications for Highway Bridges, 13th ed.*, American Association of state Highway and Transportation Officials, Washington, D.C., U.S.A.

Bardet, J.P., Ichii, K. and Lin, C.H. (2000), "EERA - A computer program for equivalent-linear earthquake site response analyses of layered soil deposits", University of Southern California, California, U.S.A.

Barka, A.A. (1996), "Slip distribution along the North Anatolian fault associated with the large earthquakes of the period 1939-1967", *Bull. Seismol. Soc. Amer.*, **86**(5), 1238-1254.

Bohnhoff, M., Martínez-Garzón, P., Bulut, F., Stierl, E. and Ben-Zion, Y. (2016), "Maximum earthquake magnitudes along different sections of the North Anatolian fault zone", *Tectonophysics*, **674**, 147-165. https://doi.org/10.1016/j.tecto.2016.02.028.

Boore, D.M., Stewart, J.P., Seyhan, E., Atkinson, G.M. (2013), "NGA-West2 equations for predicting response spectral accelerations for shallow crustal earthquakes", Pacific Earthquake Engineering Research Center (PEER), University of California, Berkeley, Berkeley, U.S.A.

Borcherdt, R.D. (1994), "Estimates of site-dependent response spectra for design (methodology and justification)", *Earthq. Spect.*, **10**(4), 617-653. https://doi.org/10.1193/1.1585791.

Bozkurt, E., (2001), "Neotectonics of Turkey", *Geodinamica Acta*, **14**(1-3), 3-30. https://doi.org/10.1080/09853111.2001.11432432.

Bürgmann, R., Ayhan, M.E., Fielding, E.J., Wright, T.J., McClusky, S., Aktuğ, B., Demir, C., Lenk, O. and Türkezer, A. (2002), "Deformation during the 12 November 1999 Düzce, Turkey, earthquakes, from GPS and InSAR data", *Bull. Seismol. Soc. Amer.*, **92**(1), 161-171. https://doi.org/10.1785/0120000834.

Campbell, K.W. (1989), "The dependence of peak horizontal acceleration on magnitude, distance, and site effects for small-magnitude earthquakes in California and Eastern North", *Bull. Seismol. Soc. Amer.*, **79**(5), 1311-1346.

Campbell, K.W. and Bozorgnia, Y. (2013), "NGA-West2 Campbell-Bozorgnia ground motion model for the horizontal components of PGA, PGV, and 5%-damped elastic pseudo-acceleration response spectra for periods ranging from 0.01 to 10 s", Pacific Earthquake Engineering Research Center (PEER), University of California, Berkeley, California, U.S.A.

Capilleri, P., Cavallaro, A. and Maugeri, M. (2014), "Static and Dynamic Characterization of Soils at Roio Piano (AQ)", *Italian Geotech. J.*, **48**(2), 38-52.

Caruso, S., Ferraro, A., Grasso, S. and Massimino, M.R. (2016), "Site response analysis in eastern Sicily based on direct and indirect Vs measurements", *Proceeding of the 1st IMEKO TC4 International Workshop on Metrology for Geotechnics*, Benevento, Italy, March.

Castelli, F., Cavallaro, A., Grasso, S. and Ferraro, A. (2016a), "In situ and laboratory tests for site response analysis in the ancient city of Noto (Italy)", *Proceedings of the 1st IMEKO TC4 International Workshop on Metrology for Geotechnics*, Benevento, Italy, March.

Castelli, F., Cavallaro, A. and Grasso, S. (2016b), "SDMT soil testing for the local site response analysis", *Proceedings of the 1st IMEKO TC4 International Workshop on Metrology for Geotechnics*, Benevento, Italy, March.

Cavallaro, A., Ferraro, A., Grasso, S. and Maugeri, M. (2008), "Site response analysis of the Monte Po Hill in the city of Catania", *AIP Conf. Proc.*, **1020**, 240-251. https://doi.org/10.1063/1.2963841.

Chen, W.F. and Scawthorn, C. (2002), *Earthquake Engineering Handbook*, CRC Press.

Cornell, C.A. (1968), "Engineering seismic risk analysis", *Bull. Seismol. Soc. Amer.*, **58**(5), 1583- 1606.

Das, S., Gupta, I.D. and Gupta, V.K. (2006), "A probabilistic seismic hazard analysis of Northeast India", *Earthq. Spect.*, **22**(1), 1-27. https://doi.org/10.1193/1.2163914.

Darendeli, M. (2001), "Development of a new family of normalized modulus reduction and material damping curves", Ph.D. Dissertation, University of Texas, Austin, Texas, U.S.A.

Deniz, A. (2006), "Estimation of earthquake insurance premium rates for Turkey", M.Sc. Thesis, Middle East Technical University, Ankara, Turkey.

Deniz, A. and Yucemen, M.S. (2010), "Magnitude conversion problem for the Turkish earthquake data", *Nat. Hazards*, **55**(2), 333-352. https://doi.org/10.1007/s11069-010-9531-8.

Dikmen, U. (2009), "Statistical correlations of shear wave velocity and penetration resistance for soils", *J. Geophys. Eng.*, **6**(1), 61-72. https://doi.org/10.1088/1742-2132/6/1/007.

EC8 (2004) EN 1998–1 (2004), "Eurocode 8: Design of structures for earthquake resistance", Part 1: General Rules, Seismic Actions and Rules for Buildings. European Committee for Standardization (CEN), Brussels, Belgium.

Edinçliler, A. and Tunçay, G.S. (2018), "Nonlinear and equivalent linear site response analysis for the Bodrum Region", *Euras. J. Civ. Eng. Architect*, **2**(2), 59-68.

El-Hady, S., Fergany, E.A.A., Othman, A. and Mohamed, G.E.A. (2012), "Seismic microzonation of Marsa Alam, Egypt using inversion HVSR of microtremor observations", *J. Seismol.*, **16**(1), 55-66. https://doi.org/10.1007/s10950-011-9249-4.

Eskişar, T., Kuruoğlu, M., Altun, S., Özyalın, Ş. and Yılmaz, H.R. (2014), "Site response of deep alluvial deposits in the northern coast of İzmir Bay (Turkey) and a microzonation study based on geotechnical aspects", *Eng. Geol.*, **172**, 95-116. https://doi.org/10.1016/j.enggeo.2014.01.006.

ESRI (2013), *ArcGIS version 10.1*, 380 New York Street, Redlands, CA 92373-8100, U.S.A.

Fatahi, B., Far, H. and Samali, B. (2014), "Soil-structure interaction vs site effect for seismic design of tall buildings on soft soil", *Geomech. Eng.*, **6**(3), 293-320. https://doi.org/10.12989/gae.2014.6.3.293.

Ferraro, A., Grasso, S., Maugeri, M., Totani, F. (2016), "Seismic response analysis in the southern part of the historic Centre of the City of L'Aquila (Italy)", *Soil Dyn. Earthq. Eng.*, **88**, 256-264. https://doi.org/10.1016/j.soildyn.2016.06.009.

Finn, W.D.L. and Ventura, C.E. (1995), "Challenging issues in local microzonation", *Proceedings of the 5th International Conference on Seismic Zonation*, Nice, France, October.

Grasso, S. and Maugeri, M. (2009), "The seismic microzonation of the city of Catania (Italy) for the maximum expected scenario earthquake of January 11, 1693", *Soil Dyn. Earthq. Eng.*, **29**(6), 953-962. https://doi.org/10.1016/j.soildyn.2008.11.006.

Gutenberg, B. and Richter, C.F. (1942), "Earthquake magnitude, intensity, energy, and acceleration", *Bull. Seismol. Soc. Amer.*, **32**, 163-191.

Gutenberg, B. and Richter, C.F. (1944), "Frequency of earthquakes in California", *Bull. Seismol. Soc. Amer.*, **34**(4), 185-188.

Gutenberg, B. and Richter, C. (1956), "Magnitude and energy of earthquakes", *Annals Geophys.*, **9**, 1-15.

Gülkan, P., Kocyigit, A., Yucemen, S., Doyuran, V. and Basoz, N. (1993), "Earthquake zoning map of Turkey based on most recent data", METU Earthquake Engineering Research Center, Ankara, Turkey.

Hanumantharao, C. and Ramana, G.V. (2008), "Dynamic soil properties for microzonation of Delhi, India", *J. Earth Syst. Sci.*, **117**, 719-730. https://doi.org/10.1007/s12040-008-0066-2.

Hardin, B.O. and Drnevich, V.P. (1972), "Shear modulus and damping in soil: Measurement and parameter effects", *J. Soil Mech. Found. Div.*, **98**(6), 603-624.

Hubert-Ferrari, A., Barka, A.A., Jacques, E., Nalbant, S., Meyer, B., Armijo, R., Tapponnier, P. and King, G.C.P. (2000), "Seismic hazard in the Marmara Sea region following the 17 August 1999 Izmit earthquake, *Nature*, **404**, 269-273. https://doi.org/10.1038/35005054.

Iyisan, R. (1996), "Correlations between shear wave velocity and penetration experiments in soils", *IMO (Technical Periodical)*, **7**, 1187-1199.

ILBANK (2015), "Karlıova municipality the basis of the zoning plan geological-geotechnical survey report", General Directorate of Bank of Provinces, Ankara, Turkey.

Joyner, W.B. and Boore, D.M. (1981), "Peak horizontal acceleration and velocity from strong-motion records including records from the 1979 imperial valley, California, Earthquake", *Bull. Seismol. Soc. Amer.*, **71**(6), 2011-2038.

Kalafat, D., Pınar, A., Kuleli, S., Gülen, L. and Toksöz, N. (2006), "12, 14, 23 Mart (Mw=5.4, Mw=5.9, Mw=5.4), 6 Haziran 2005 (Mw=5.7) ve 2 Temmuz 2006 (Mw=4.9) The sequence of Karlıova-Bingöl earthquakes", *Proceedings of the Active Tech. Arş Group 10th Meeting*, İzmir, Turkey, November.

Kalkan, E., Gülkan, P., Yilmaz, N. and Çelebi, M. (2009), "Reassessment of probabilistic seismic hazard in the Marmara Region", *Bull. Seismol. Soc. Amer.*, **99**(4), 2127-2146. https://doi.org/10.1785/0120080285.

Kallberg, K.T. (1969), "Seismic risk of Southern California", M.I.T. Research Report R69-31, Department of Civil Engineering, Massachusetts Institute of Technology, Cambridge, Massachusetts, U.S.A.

Kienzle, A., Hannich, D., Wirth, W., Ehret, D., Rohn, J., Ciugudean, V. and Czurda, K. (2006), "A GIS-based study of earthquake hazard as a tool for the microzonation of Bucharest", *Eng. Geol.*, **87**(1-2), 13-32. https://doi.org/10.1016/j.enggeo.2006.05.008.

Kijko, A. and Graham, G. (1998), "Parametric-historic procedure for probabilistic seismic hazard analysis Part I: Estimation of maximum regional magnitude m max", *Pure Appl. Geophys.*, **152**(3), 413-442. https://doi.org/0033–4553/98/030413–30.

Kolat, C., Ulusay, R. and Suzen, M.L. (2012), "Development of geotechnical microzonation model for Yenisehir (Bursa, Turkey) located at a seismically active region", *Eng. Geol.*, **127**, 36-53. https://doi.org/10.1016/j.enggeo.2011.12.014.

Kramer, S.L. (1996), *Geotechnical Earthquake Engineering*, Prentice Hall, Upper Saddle River, New Jersey, U.S.A.

Kramer, S. (2009a), "CEE 526 Geotechnical Earthquake Engineering lecture notes", University of Washington, Seattle, Washington, U.S.A.

Midorikawa, S. (1987), "Prediction of isoseismal map in Kanto plain due to hypothetical earthquake", *J. Struct. Dyn.*, **33**, 43-48.

Nalbant, S., Mc Closkey, J., Steacy, S. and Barka, A. (2002), "Strees accumulation and increased seismic risk in eastern Turkey", *Earth Planet. Sci. Lett.*, **195**(3-4), 291-298. https://doi.org/10.1016/S0012-821X(01)00592-1.

NEHRP-BSSC (2003), "NEHRP (National Earthquake Hazard Reduction Program) recommended provisions for New buildings and other structures (FEMA 450)", Building Seismic Safety Council, National Institute of Building Sciences, Washington, D.C., U.S.A.

NTC (2008), "Norme Tecniche per le Costruzioni (Italian Technical Regulation for Constructions)", D.M. Ministero Infrastrutture e Trasporti 14 gennaio. Roma, Italy.

Ordonez, G. (2012), "Shake2000: A computer program for the 1-D analysis of geotechnical earthquake engineering problems", GeoMotions, LLC, Washington, U.S.A.

Ozalp, S., Dogan, A. and Emre, O. (2005), "6 June 2005 Evaluation of the Karlıova Earthquake", MTA Geological Studies Department, Earth Dynamics Research and Evaluation Coordinator Active Tectonic Research Unit.

Ozbey, C., Sari, A., Manuel, L., Erdik, M. and Fahjan, Y. (2004), "An empirical attenuation relationship for Northwestern Turkey ground motion using a random effects approach", *Soil Dyn. Earthq. Eng.*, **24**(2), 115-125. https://doi.org/10.1016/j.soildyn.2003.10.005.

PEER (2019), Pacific Earthquake Engineering Research Center, Strong Motion Database, https://ngawest2.berkeley.edu.

Reilinger, R.E., McClusky, S.C., Oral, M.B., King, W. and Toksöz, M.N. (1997), "Global Positioning System measurements of present-day crustal movements in the Arabian-Africa-Eurasia plate collision zone", *J. Geophys. Res.*, **102**(B5), 9983-9999. https://doi.org/10.1029/96JB03736.

Richter, C.F. (1958), *Elementary Seismology*, W.H. Freeman, London, U.K.

Robertson, P.K., Woeller, D.J. and Finn, W.D.L. (1992), "Seismic cone penetration test for evaluating liquefaction potential under cyclic loading", *Can. Geotech. J.*, **29**(4), 686-695. https://doi.org/10.1139/t92-075

Saroglu, F., Emre, O. and Kuscu, I. (1992), "The East Anatolian fault zone of Turkey", *Annales Tectonicae*, **7**, 99-125.

Seed, H. and Idriss, I. (1981), "Evaluation of liquefaction potential sand deposits based on observation of performance in previous earthquakes", *Proceedings of the ASCE National Convention (MO)*, St. Louis, Missouri, U.S.A., October.

Seed, H.B., Wong, R.T., Idriss, I.M. and Tokimatsu, K. (1986), "Moduli and damping factors for dynamic analyses of cohesionless soils", *J. Geotech. Eng.*, **112**(11), 1016-1032. https://doi.org/10.1061/(ASCE)0733- 9410(1986)112:11(1016).

Selçuk, L. and Çiftçi, Y. (2007), "Microzonation of the Plio-Quaternary soils: a study of the liquefaction risk potential in the Lake Van Basin Turkey", *Bull. Eng. Geol. Environ.*, **66**(2), 161-176. https://doi.org/10.1007/s10064-006-0052-3.

Shafiee, A., Kamalian, M., Jafari, M.K. and Hamzehloo, H. (2011), "Ground motion studies for microzonation in Iran", *Nat. Hazards*, **59**(1), 481-505. https://doi.org/10.1007/s11069-011-9772-1.

Shiuly, A. and Narayan, J.P. (2012), "Deterministic seismic microzonation of Kolkata city", *Nat. Hazards*, **60**(2), 223-240. https://doi.org/10.1007/s11069-011-0004-5.

Sitharam, T.G. and Anbazhagan, P. (2007), "Seismic Hazard Analysis for the Bangalore Region", *Nat. Hazards*, **40**(2), 261-278. https://doi.org/10.1007/s11069-006-0012-z.

Sonmezer, Y.B., Akbas, S.O. and Isik, N.S. (2015), "Assessment of the peak acceleration, amplification ratio and fundamental period properties for the Kirikkale province settlement area", *J. Fac. Eng. Archit. Gazi Univ.*, **30**(4), 711-721.

Sonmezer, Y.B., Bas, S., Isik, N.S. and Akbas, S.O. (2018),

"Linear and nonlinear site response analyses to determine dynamic soil properties of Kirikkale", *Geomech*. *Eng*., **16**(4), 435-448.
https://doi.org/10.12989/gae.2018.16.4.435.

Sonmezer, Y.B., Celiker, M. and Bas, S. (2019), "An investigation on the evaluation of dynamic soil characteristics of the Elazig City through the 1-D equivalent linear site-response analysis", *Bull*. *Eng*. *Geol*. *Environ*., **78**(7), 4689-4712. https://doi.org/10.1007/s10064-018-01450-6.

Sun, J., Golesorkhi, R. and Seed, H. (1988), "Dynamic moduli and damping ratios for cohesive soils", Earthquake Engineering Research Center, Berkeley, California, U.S.A.

Tavakoli, H., Amiri, M., Abdollahzadeh, G. and Janalizade, A. (2016), "Site effect microzonation of Babol Iran", *Geomech*. *Eng*., **11**(6), 821-845.
https://doi.org/10.12989/gae.2016.11.6.82.1

Toksöz, M.N., Shakal, A.F. and Michael, A.J. (1979), "Space-time migration of earthquakes along the North Anatolian Fault Zone and seismic gaps", *Pure Appl*. *Geophys*., **117**(6), 1258-1270.

TEC (2018), "Turkish earthquake code for buildings", Disaster and Emergency Management Directorate; Ankara, Turkey.

Tunç, B., Güven, T., Ulutaş, E., Irmak, T.S., Sertçelik, F., Çetinol, T., Çaka, D., Özer, M.F. and Edge, Ö. (2003), "Experimental largest horizontal acceleration distance decrease relationship for the Eastern Marmara Region and the probalistic earthquake hazard of Kocaeli", *Proceedings of the Earthquake Symposium*, Kocaeli, Turkey.

Unutmaz, B., Siyahi, B., Fahjan, Y. and Akbaş, B. (2011), "Derin alüvyon dolgunun doğrusal olmayan davranışının eşdeğer lineer ve doğrusal olmayan yöntemlerle karşılaştırılması", *Proceedings of the 1. Türkiye Deprem Mühendisliği ve Sismoloji Konferansı*, Ankara, Turkey.

Ulusay, R., Tuncay, E., Sonmez, H. and Gokceoglu, C. (2004), "An attenuation relationship based on Turkish strong motion data and iso-acceleration map of Turkey", *Eng*. *Geol*., **74**(3), 265-291. https://doi.org/10.1016/j.enggeo.2004.04.002.

Vucetic, M. and Dobry, R. (1988), "Degradation of marine clays under cyclic loading", *J. Geotech*. *Eng*., **114** (2), 133-149. https://doi.org/10.1061/(ASCE)0733-9410(1988)114:2(133).

Vucetic, M. and Dobry, R. (1991), "Effect of soil plasticity on cyclic respons", *J. Geotech*. *Eng*., **117**(1), 89-107. https://doi.org/10.1061/(ASCE)0733-9410(1991)117:1(89).

Yücemen, M.S. (2011), "Probabilistic seismic hazard analysis: Overview and next generation earthquake hazard maps", *Proceedings of the 7th National Earthquake Engineering Conference*, Istanbul, Turkey.

CC